A new approach to finding optimal centrifugation conditions for shear-sensitive microalgae

A. Molina-Miras, L. López-Rosales, M. C. Cerón-García, A. Sánchez-Mirón, F. García-Camacho, A. Contreras-Gómez*, E. Molina-Grima

Department of Chemical Engineering, University of Almería, 04120, Almería (Spain)

* Author for correspondence

Department of Chemical Engineering

University of Almería

04120 Almería, Spain

e-mail: acontre@ual.es

Abstract

A study has been conducted to assess clarification efficiency and cell damage during centrifugation, and to optimize this operation for the dinoflagellate microalga *Amphidinium carterae*. Although cells were easily recovered from the cell suspension, cell damage was observed in some experiments once the cells had sedimented. Cell damage depends on both the residence time of the cells in the pellet and on the g-force applied. 2D CFD simulations were carried out to simulate and predict microalgal cell settling times, and a dimensionless number was used to obtain an operating window (combinations of g-force and centrifugation time) for optimal centrifugation of the microalga. The approach used in this study can be extrapolated to other cells and other centrifuges.

2

1. Introduction

Microalgae have been traditionally used as food for larval and juvenile animals in aquaculture [1]. However, nowadays, they are also attracting enormous interest due to their vast potential in a large variety of other applications, for example in wastewater treatment and sequestration of atmospheric CO_2 [2], production of biofuels (mainly biodiesel) as promising alternatives to fossil fuels in terms of economic, renewability, and environmental concerns [3], and production of numerous high-value compounds, including polyunsaturated fatty acids, antioxidants, vitamins, and antimicrobial and anticancer drugs [4].

Marine dinoflagellates are an intriguing class of microalgae (class Dinophyceae) that are known to produce a range of fascinating bioactive compounds [5-6]. For example, the dinoflagellate *Amphidinium carterae* produces an interesting group of polyketide metabolites, namely amphidinolides and amphidinolds (both referred to henceforth as APDs), which elicit potent anticancer, antifungal and haemolytic activities and are therefore potentially useful in studies of drug design [7]. As such, the demand for increasing quantities of APDs, as well as other dinoflagellate-derived bioactive compounds, is increasing [6]. However, the only source of APDs is currently APD-producing microalgae, and supply constraints are a major obstacle to the successful research, development, and marketing of these compounds [5-6, 8]. In recent studies, the feasibility of producing bioactive substances from pilot-plant cultures of the dinoflagellates *A. carterae* and *Karlodinium veneficum* using simple and scalable processes has been assessed [9-13].

Despite the huge potential of microalgae in general, and dinoflagellates in particular, in a wide range of applications, microalgal-based production systems for high-value

3

bioactives are not yet economically viable. Different upstream strategies to improve the

economics of these processes have been discussed extensively, including the use of

genetically modified strains [14], the use of wastewater as a culture medium to reduce

both the freshwater requirement and production costs [3, 15], and the implementation of

biorefinery-based production strategies, taking advantage of every component of the

microalgal biomass to obtain useable products in order to lower overall production costs

[16, 17]. However, despite the progress made in microalgal cultivation systems, the

final concentration of biomass when grown phototrophically is very low (less than 1 gL^{-1} for open ponds and about 5 gL^{-1} for closed systems), with small cell sizes (5-30 μm)

and cell densities close to that of water (average ~ 1020 kg m^{-3}) [16]. As such, large

volumes of algal suspensions need to be handled in downstream processing.

Harvesting of the biomass from the broth is considered a critical step and has been

estimated to account for up to 30% of the total cost of microalgae production [18]. As

such, the implementation of energy-efficient and cost-effective technologies and

protocols for effective separation and recovery is imperative [19]. Microalgal harvesting

relies on reducing the water content of the microalgal suspension as much as possible.

Moreover, an ideal separation process should be applicable to most strains of

microalgae, provide a product biomass with a high dry weight, and require reduced

energy, operating and maintenance costs. Amongst others, the processes commonly

used to harvest microalgae include screening, flocculation, sedimentation, filtration, and

centrifugation. Although it is generally accepted that there is currently no definitive and

highly efficient harvesting method that can be used with all microalgal strains, it is

widely accepted that centrifugation is the fastest method, is applicable to the vast

majority of microalgae and, in many cases, can be used as a one-step separation process

[18, 20].

4

Centrifugation is routinely used for research and small-scale operations, and for the recovery of high-value metabolites. Nonetheless, although the reliability and efficiency of centrifugation are high, evidence that high shear rates and centrifugal forces can potentially result in cell damage [13, 21], and operating costs [20], frequently offset its merits for large-scale algal separation.

Centrifuges are normally adjusted to maximize recovery efficiency. However, recovery efficiency depends on the settling characteristics of the cell, centrifuge design, and the centrifugation protocol (settling depth, retention time, and centrifugal force). As such, the highest recovery efficiency may not coincide with cost-effective and damage-free algal cell harvesting.

Herein we introduce an approach based on a dimensionless number to develop cell damage free centrifugation protocols for shear-sensitive microalgae. The model microalga used was *A. carterae* and the procedure was corroborated using literature data for a microalga lacking a cell wall (*Dunaliella salina*) and for an extremely shear-sensitive cell (*Spodoptera exigua*). Our findings corroborate that the approach presented in this work may be useful for developing reliable centrifugation protocols, thereby avoiding cell damage.

2. Materials and Methods

2.1. The microalga and maintenance

Monocultures of the marine dinoflagellate microalga *A. carterae* (strain Dn241EHU) were used. The strain was provided by the Culture Collection of the Plant Biology and Ecology Department at UPV (Spain). *A. carterae* inocula were grown in flasks at 21 ± 1

°C under a 12:12 h light–dark cycle. The irradiance at the surface of the culture flasks

(60 µE m^{-2} s^{-1}) was provided by four 58 W fluorescent lamps. f/2 medium with an N:P

molar ratio of 24 [22, 23] was used for inoculum maintenance.

2.2. Centrifugation assays

Cultures for centrifugation experiments were obtained by inoculating cells in

exponential growth phase in a 10-liter bubble column photobioreactor, as described

elsewhere [24]. Briefly, the culture medium was a modification of f/2 with an N:P

molar ratio of 5 [13], and the culture temperature was maintained at 21±1 °C under a

12:12 h light–dark cycle irradiance at the surface (600 µE m^{-2} s^{-1}). Cultures were

sparged continuously with filtered air at a flow rate of 0.5 vvmin, and the pH was

maintained at 8.5 by automatic on-demand injection of pure carbon dioxide.

Microalgal cultures at a cell concentration of 4.0×10^6 cells mL^{-1} and with a viability of

more than 98% were used in all experiments. Cell concentration and viability were

quantified by flow cytometry, as described elsewhere [11]. Five measurements per

sample were performed and the average value was used. The mean cell equivalent

diameter was 12.39±0.78 µm (n=105). Since *A. carterae* cells have an ellipsoidal shape

[25], the equivalent diameter was used to calculate the longest ($L = 22$ µm),

intermediate ($I = 12$ µm), and shortest ($S = 7$ µm) lengths of the cells.

Cultures were deposited in 50 mL Falcon tubes and centrifuged in a benchtop centrifuge

(Beckman Coulter, model Allegra 25R) using a rotor (swing-out head) with a maximum

radius of 13.7 cm (max RCF = 15300×g). The height of the suspension (h_c) was 10.4 cm

throughout the experimental work; g-forces (g_c) of up to 13500×g, and centrifugation

times (t_c) of up to 35 min were used. After centrifugation, the supernatant was removed

6

and the cell pellet was re-suspended in fresh medium. Cell concentration was measured using a hemocytometer under a light microscope, and cell viability was estimated using chlorophyll as a marker for cell rupture. The relationship between broken cell and chlorophyll concentration was obtained as follows: A volume of 100 mL of cell suspension was sonicated on ice using an ultrasonic probe-type device (Hielscher Ultrasonics, model UP200S) with the following settings: 0.5 pulse cycle, 80% amplitude. The extent of cell rupture was checked by light microscopy. All cells were broken after 6 minutes. After sonication, the samples were centrifuged (3000×g, 8 min) to remove cell debris, and serial dilutions were prepared using the culture medium as diluent. Volumes of 200 µL of solution were placed in a black, clear-well, flat-bottomed 96-well microplate (Corning, ref 3603) to prevent well-to-well crosstalk, and the fluorescence of chlorophylls was measured using a monochromator-based microplate reader (BioTek, model Synergy Mx). The excitation wavelength was 480 nm and emission wavelengths were between 500 and 700 nm. The area below the emission curve between 640 and 800 nm was related to broken cells, as shown in Fig. 1.

The cell density was measured by density gradient centrifugation in Percoll according to the method described by Whitelam et al. [26]. A value of 1200 g mL^{-1} was obtained. The bulk density of the culture medium was measured using a pycnometer and found to be 1037 g mL^{-1}. The viscosity of suspensions was measured using a viscometer (Brookfield, model DV-II+Pro) and found to be 1180×10^{-6} Pa s. No significant changes in these parameters were observed for the different cultures.

The efficiency of the centrifugation process (η_c) was defined as

$$\eta_c = \frac{N_p}{N_i} \qquad (1)$$

where N_p and N_i are the total number of cells in the pellet and in suspension prior to

414
415
416
417
418
419
420
421
422
423
424
425
426
427
428
429
430
431
432
433
434

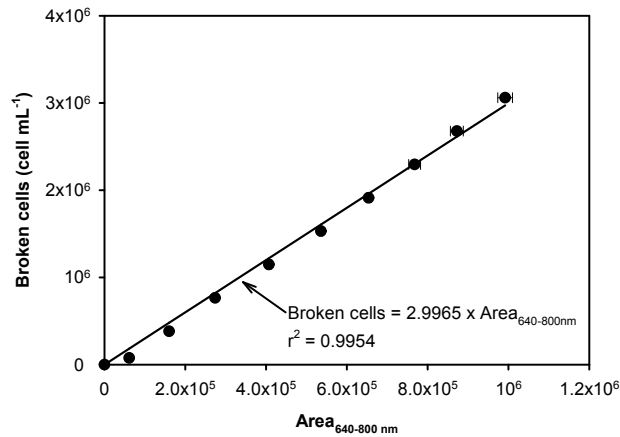treatment, respectively. All experiments were carried out in duplicate.

Fig. 1. Relationship between broken *A. carterae* cell concentration and the area below

the chlorophyll emission curve between 640 and 800 nm, after excitation at 480 nm.

The equation allows the estimation of cell viability after centrifugation experiments.

The experimental data are represented as the average for duplicate experiments ±

standard deviation.

2.3. CFD simulations

Cell-sedimentation times for each centrifugation experiment were simulated using the

CFD software Fluent® v19.2 (Ansys, Canonsburg, PA, USA). As the tube is axis-

symmetrical, it was simulated in 2D using a structured grid with an optimum size of 0.2

mm. Laminar flow was assumed and a two-phase Eulerian model, in which the cells

represent the granular phase, was used to describe the solid-liquid interactions. The

initial cell volume fraction in the suspension was 0.00458, as calculated from the cell

diameter and the cell concentration in suspension. No energy balance was imposed, as

isothermal conditions were assumed. The reference for pressure was at the top of the

suspension. Boundary conditions included non-slip conditions at the walls. The schemes

8

used for spatial discretization were second -order upwind for momentum, Green-Gauss Node Based for gradient and Modified HRIC for volume fraction. The SIMPLE scheme with implicit formulation was chosen for pressure-velocity coupling. All simulations in the present study were performed in transient mode using a time step of 0.0005 s. The convergence criteria were checked at every time-step and residuals for all the variables were fixed at 10^{-5}. An HP Z840 Workstation with two Intel® Xeon E5-2670 v3 processors running at 2.3 GHz with 128.0 GB RAM and 3 TB×2 hard disks was used for the simulations [27].

3. Results and Discussion

3.1. The approach

Despite the critical relevance of the operating parameters (mainly h_c, t_c, and g_c) on the output of discontinuous centrifugation, the performance of a centrifugation operation for harvesting microalgae and other cells or microorganisms is usually expressed in qualitative terms [28], and a wide variety of centrifugation protocols, with different suspension heights, times, and centrifugal forces, are used for no specific reason [29]. Indeed, they are frequently selected arbitrarily as the same separation can be achieved with different combinations of parameters. However, it is widely accepted that the conditions required to achieve complete cell separation can potentially damage cells, particularly in the case of shear-sensitive cells. The origin of this cell damage has been mainly related to hydrodynamic shear forces associated with the velocity gradients, relative cell-fluid movement during settlement, and the compressive centrifugal forces to which cells are submitted in the pellet. As such, the time that cells remain in the pellet, and the g-force applied, are critical parameters determining cell survival in

centrifugation processes. Indeed, the longer the cells remain in the pellet, the longer the compressive forces act, eventually producing cell damage [30, 31]. It has also been shown that long periods of time in the pellet may also result in severe cell deterioration or even death due to the exhaustion of essential nutrients [32].

Despite all the efforts made in the past, quantification of the impact of varying centrifugation parameters on the performance of centrifugation, especially when fragile biological materials are used, is currently not possible [31, 33]. Nonetheless, a quantitative approach can provide a deeper insight into centrifugation performance and the effect on cells. This work uses a new approach to study the influence of centrifugation parameters on separation efficiency capacity and cell damage. This approach allows the operating conditions for complete separation and operating conditions that lead to cell damage to be determined, thus providing an "operating window" for a specific cell in a particular centrifuge, as discussed below. This approach uses a dimensionless number, namely the centrifugation number (Ce), which is equivalent to a dimensionless time, to represent the intensity of the treatment. It is defined as:

$$Ce = \frac{t_c}{t_s} \qquad (2)$$

where t_c is the centrifugation time and t_s is the sedimentation time. If the time taken for acceleration and deceleration of the rotor is neglected, t_c represents the time that the cells are subjected to centrifugal forces. t_s is the time needed to sediment all the cells. t_c is an operating variable and t_s can easily be determined from experimental data. If no experimental t_s values are available, a theoretical value of t_s can be estimated from h_c and the settling velocity.

10

According to the theory of particle movement through a fluid, the terminal settling

velocity of a small particle in dilute suspension under gravity is given by [34]:

$$v = \sqrt{\frac{2\,g(\rho_s - \rho)m_s}{A\,\rho_s\,C_D\,\rho}} \qquad (3)$$

where v is the sedimentation velocity under gravity, g is the gravitational acceleration,

ρ_S is the density of the particle, ρ is the density of the fluid, m_s is the mass of the

particle, A is the projected area of the particle (the area obtained projecting the particle

on a plane perpendicular to the line of flow), and C_D is the drag coefficient. In a

centrifuge, the corresponding terminal velocity is:

$$v_c = \sqrt{\frac{2\omega^2 r(\rho_s - \rho)m_s}{A\rho_s C_D\rho}} = \sqrt{\frac{2\,g_c(\rho_s - \rho)m_s}{A\,\rho_s\,C_D\,\rho}} \qquad (4)$$

where ω is the angular velocity, r is the radius of the centrifuge, and g_c is the g-force,

the force developed in a centrifuge relative to the force of gravity. For spherical

particles, equation (4) can be written as:

$$v_c = \sqrt{\frac{4g_c(\rho_s - \rho)D_s}{3C_D\rho}} \qquad (5)$$

where D_s is the diameter of the particle. The drag coefficient for spherical particles is a

function of the particle Reynolds number Re, and in laminar flow can be written as [34]:

$$C_D = \frac{24}{Re} = \frac{24}{\dfrac{D_s v_c \rho}{\mu}} \qquad (6)$$

where μ is the viscosity of the liquid. Substituting this into equation (5) gives the

following equation:

$$v_c = v_{Stokes} = \frac{g_c D_s^2 (\rho_s - \rho)}{18\mu} \tag{7}$$

known as Stokes' law.

Hence, for spherical particles in dilute solutions, if no experimental t_s values are available, the theoretical t_s can be estimated from h_c and Stokes' settling velocity as:

$$t_s = \frac{h_c}{v_{Stokes}} = \frac{18\mu h_c}{g_c D_s^2 (\rho_s - \rho)} \tag{8}$$

Substituting Eq. (8) into Eq. (2) gives the following expression for Ce:

$$Ce = \frac{t_c}{t_s} = a\frac{g_c t_c}{h_c} \tag{9}$$

where a is a constant for a particular cell-fluid system given by:

$$a = \frac{D_s^2 (\rho_s - \rho)}{18\mu} \tag{10}$$

For non-spherical particles, general equation (4) can be used to estimate sedimentation velocity. Numerous correlations can be found in the literature to estimate C_D for different particles, with one of the most recent correlations for estimating the average drag coefficient of freely falling solid non-spherical particles in liquids or gases being proposed by Bagheri and Bonadonna [36], modifying Eq. (6):

$$\frac{C_D}{k_N} = \frac{24\,k_S}{Rek_N}\left(1 + 0.125\left(Re^{k_N/k_S}\right)^{2/3}\right) + \frac{0.46}{1 + 5330\big/\left(Re^{k_N/k_S}\right)} \tag{11}$$

where

$$k_S = \left(F_S^{1/3} + F_S^{-1/3}\right)/2 = 1.101$$

$$k_N = 10^{\alpha_2[-log(F_N)]\beta_2} = 0.936$$

$$\alpha_2 = 0.45 + {}^{10}/exp(2.5\ log\rho' + 30) = 0.45$$

$$\beta_2 = 1 - {}^{37}/exp(3\ log\rho' + 100) = 1$$

and

$$F_S = fe^{1.3} = 0.263$$

$$F_N = f^2\ e = 0.191$$

where e is the elongation (I/L) and f the fatness (S/I). L, I, and S are the longest, the

intermediate, and the shortest length of the particle, respectively; and ρ' is the particle-

to-fluid density ratio. Eq. (11) is based on dimensional analysis, by normalizing the drag

coefficient and particle Reynolds number, and has been shown to be valid for any

particle shape and any normalized Reynolds number [36].

A high particle concentration negatively affects particle settling velocity in a

suspension, and different models have been proposed over the past 100 years or so to

predict the settling velocity for different particles in concentrated suspensions [37],

although the prediction of sedimentation times under these conditions remains

complicated. In this scenario, CFD can also be successfully used to predict

sedimentation times. Thus, in this work, the Bagheri and Bonadonna equation [36] was

incorporated into a user-defined function to modify the drag force in Fluent to estimate

the theoretical t_s.

As pointed out above, the dimensionless number used in this approach, Ce, represents

the intensity or magnitude of the centrifugation treatment. If $Ce = 1$, we have an "ideal

treatment" where t_c equals t_s, all the cells are separated and the mean time that cells

13

remain in the pellet approaches 0. If $Ce < 1$, we have a "deficiency of treatment" and

not all the cells sediment. If Ce is > 1, we have an "excess of treatment". In this case, all

the cells are separated, but the time that the cells remain in the pellet is > 0 and, if the

process lasts too long, it will potentially be deleterious for cells at some point. This

approach provides an "operating window" for optimal centrifugation of a particular cell-

centrifuge system, as discussed below for three different cells in three different

centrifuges.

3.2. Application to Amphidinium carterae cells

The clarification efficiency for representative g-forces up to 2000×g used in this work is

shown in Fig. 2. As can be seen, the longest time needed to recover all the cells (15

min) was obtained for the lowest g_c (100×g). As g_c increased, the time needed for

complete cell separation decreased, reaching roughly 1 min at 2000×g.
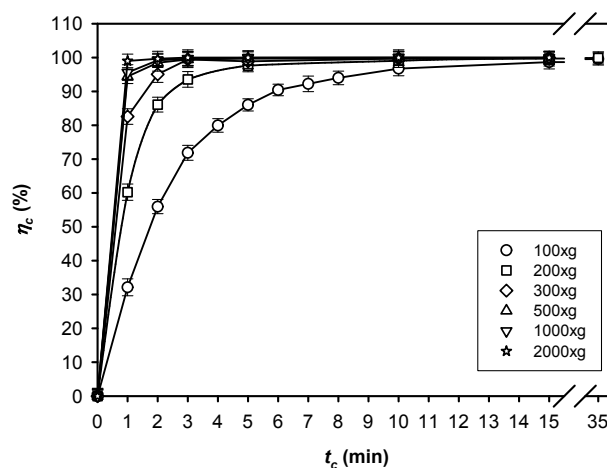
Fig. 2. Centrifugation of *A. carterae* cells. Influence of centrifugation time (t_c) on the

clarification efficiency (η_c) for different centrifugation forces (g_c). For clarity, only

experiments up to 2000×g are shown. The experimental data are represented as the

14

average for duplicate experiments ± standard deviation.

The experimental t_s values derived graphically from the data presented in Fig. 2, as the time needed to reach a separation efficiency of 100% for the different g_c values, are shown in Fig. 3.
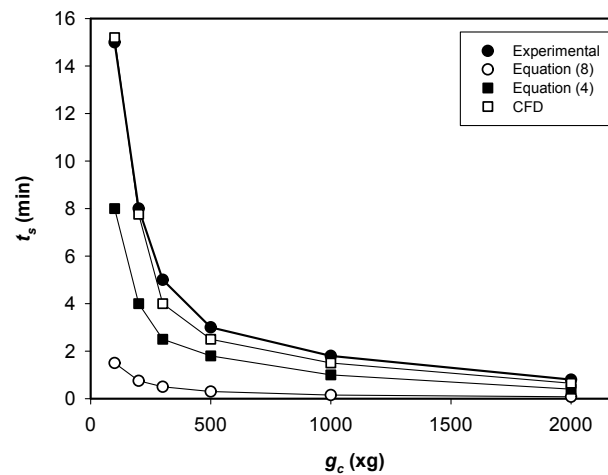

Fig. 3. Influence of g_c on sedimentation time (t_s) of *A. carterae* cells. Experimental times are derived graphically from Fig. 2. Theoretical values of t_s predicted using Eq. (8), Eq. (4), and CFD are also shown.

The values obtained for t_s using equation (8) and (4) are also shown in Fig. 3. As stated above, the application of Stokes' equation implies several assumptions for the behavior of the cells, with the most relevant being: spherical particles, laminar flow, and the particles do not interfere with each other during the settling process. As can be seen from Fig. 3, Stokes' equation greatly underestimates sedimentation times and therefore should not be used to describe sedimentation of *A. carterae* cells. Since the calculated *Re* number reveals that the flow remained in the laminar region for all experiments (data not shown), this significant discrepancy between the sedimentation times obtained using

15

Stokes' equation and the experimental values may be due to the morphology of the *A. carterae* cell, which presents the typical shape of the *Amphidinium* genus, namely oval in ventral view and dorso-ventrally flattened, with two flagella, or to the interference of cells with each other during the settling process.

The morphology of the cells undoubtedly negatively affects sedimentation. As such, to take cell shape into account, the general equation for terminal velocity (Eq. (4)) with C_D obtained from Eq. (11) was also used to predict settling velocities. It is clear that although Eq. (4) improves the prediction of Stokes' equation, predicted t_s values are still about 50% lower than experimental times (see Fig. 3). In this scenario, CFD was also used to predict t_s. Thus, the Bagheri and Bonadonna equation [36] was incorporated into a user-defined function to modify the drag force in Fluent.

As can be seen in Fig. 3, CFD provided t_s values very close to the experimental ones. The minor discrepancies observed are probably due to the lack of precision in the graphical determination of experimental t_s [31]. These results support the use of CFD as a solid and useful tool for predicting sedimentation times for single-cell suspensions in discontinuous centrifugation without the need for experimentation. As such, CFD was also used to predict t_s for g-forces over 2000×g because settling times over this g-force were below the minimum working time of the centrifuge (1 minute).

Fig. 4a shows the separation efficiency (η_c) and percentage of viable cells (V_c) versus Ce for all experiments. It can be seen from this figure that, for $Ce < 1$, η_c increases linearly to reach its highest value (100%) at a Ce value of 1. For higher Ce values up to 80, η_c remains constant, subsequently decreasing sharply due to cell rupture for Ce > 80. V_c, in turn, is close to 100% up to a Ce value of 80, whereas for $Ce > 80$, V_c also decreases sharply due to cell rupture in a similar manner to η_c. In this scenario, a Ce

16

945
946
947
948
949
950
951
952
953
954
955
956
957
958
959
960
961
962
963
964
965
966
967
968
969
970
971
972
973
974
975
976
977
978
979
980
981
982
983
984
985
986
987
988
989
990
991
992
993
994
995
996
997
998
999
1000
1001
1002
1003

value of 80 is the "critical Ce" and represents the maximum magnitude of treatment that
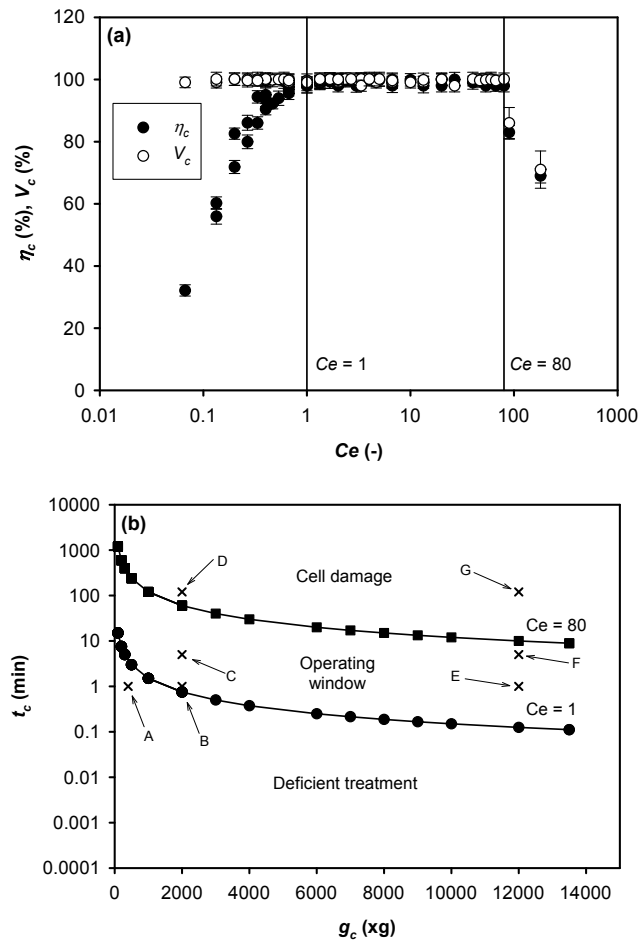
A. carterae cells can withstand in this centrifuge.

17

1004
1005
1006
1007
1008
1009
1010
1011
1012
1013
1014
1015
1016
1017
1018
1019
1020
1021
1022
1023
1024
1025
1026
1027
1028
1029
1030
1031
1032
1033
1034
1035
1036
1037
1038

Fig. 4. Separation efficiency (η_c) and cell viability (V_c) for different centrifugation

numbers (*Ce*) (a), and operating window (b), for *A. carterae* cells centrifugation. *Ce* =

1 is the *Ce* value for complete cell separation and *Ce* = 80 is the "critical *Ce*", the *Ce*

value above which cell integrity is compromised. The separation efficiency and cell

viability data are represented as the average for duplicate experiments ± standard

deviation. See text for further details.

These data can be rearranged as shown in Fig. 4b, which shows the operating window

(values of t_c and g_c) for this cell. All combinations of t_c and g_c inside the operating

window will give complete cell separation with no cell damage. For combinations

18

below the line representing $Ce = 1$, the treatment will be deficient and not all cells will
be separated. For combinations over the line of $Ce = 80$, cells will be damaged.

To corroborate the applicability of this approach, a new set of experiments was carried
out under different centrifugation conditions. These experiments are shown in Fig. 4b
(points A to G). In experiment A (400×g, 1 min) a η_c of 90% was obtained, with a V_c of
99%. This experiment represents a deficient treatment and clearly lies outside the
operating window. In experiments B (2000×g, 1 min) and C (2000×g, 5 min), a η_c of
100% with a V_c of 98% and 99%, respectively, was obtained. These two points are
clearly inside the operating window and represent optimal centrifugation conditions.
However, in experiment D (2000×g, 120 min) η_c and V_c decreased to 90% due to cell
rupture. This experiment represents an excessive treatment and is clearly outside the
limits of the operating window. Similar results were obtained in experiments carried out
at 12,000×g. Thus, in experiments E (12000×g, 1 min) and F (12000×g, 5 min), a η_c of
100% was obtained, with a V_c of 99% in both cases, whereas in experiment G
(12,000×g, 120 min) both η_c and V_c decreased to 60%.

As noted in section 2.2, the height of the suspension in the centrifuge tubes was 10.4 cm
in all experiments carried out in this work. According to Eq. (9), if the height of the
suspension changes, g_c or t_c, or both, have to change in order to keep Ce constant. This
implies that a change in the height of the suspension would produce a displacement of
the operating window to higher or lower values of g_c, t_c, or both, while keeping the
width of the operating window constant.

To corroborate the applicability of the Ce number approach discussed above to different
cell-centrifuge systems, it was applied to centrifugation data from the literature for a

19

microalga lacking a cell wall (*Dunaliella salina*; [21]) and to the very shear-sensitive

Spodoptera exigua Se301 cell line [31].

3.3. Application to Dunaliella salina cells

Recently, Xu et al. [21] used mechanistic calculations to explore the potential cell

damage that may result due to different forces acting on *Dunaliella salina* cells during

centrifugation in a benchtop microcentrifuge (Eppendorf, model 5415R) using a fixed-

angle rotor at different g-forces (from 1000 to 15,000×g) for a fixed time (10 min). The

authors assumed a spherical shape with a diameter of 10 μm for *Dunaliella* cells and

that Stokes' law (Eq. 7) was applicable. Calculations included hydrodynamic stress due

to turbulence, viscous drag, hydrostatic pressure exerted on cells at the bottom of the

centrifuge tube, the pressure acting on the cells due to their own mass and the

centrifugal force, and the pressure of the cells in the pellet acting on the cells at the

bottom of the pellet. They concluded that *D. salina* cell rupture observed for g-forces

over 5000×g was due to the hydrostatic pressure, with the other forces being

considerably lower than those estimated to be required for cell rupture [21].

To apply the *Ce* number approach to these experiments, the same assumptions

(spherical cells and Stokes' law applicable) were applied. CFD could not be used due to

a lack of geometrical data for the centrifuge rotor and centrifuge tube, and the absence

of experimental values for t_s. Fig. 5a shows that, with those assumptions, the *Ce* used in

these experiments were thousands of times higher than that needed for complete

separation of *Dunaliella* cells (*Ce* = 1). Indeed, cell rupture, with a sharp decline in V_c,

was observed for *Ce* values over 5600. This provides a very large operating window, as

seen in Fig. 5b. According to the authors, in the experiment carried out at 3000×g,

20

100% cell separation, with a V_c of 100%, was obtained. It can be seen from Fig. 5b that

these centrifugation conditions (3000×g, 10 min) are inside the operating window (point

A). The authors point out that the number of intact cells present in the pellet decreased

upon increasing g_c above 5000×g. These results are clearly corroborated in Fig 5b,

which shows that g_c = 5000×g and t_c = 10 min are in the limit of the operating window

(point B), and that increasing g_c over 5000×g is expected to result in an increasing

number of cells being damaged, as observed by the authors in experiments at g_c =

9000×g, where V_c for the pellet decreased to 60%. As can be seen from Fig 5b, the

combination 9000×g and 10 min clearly lies outside the operating window (point C).
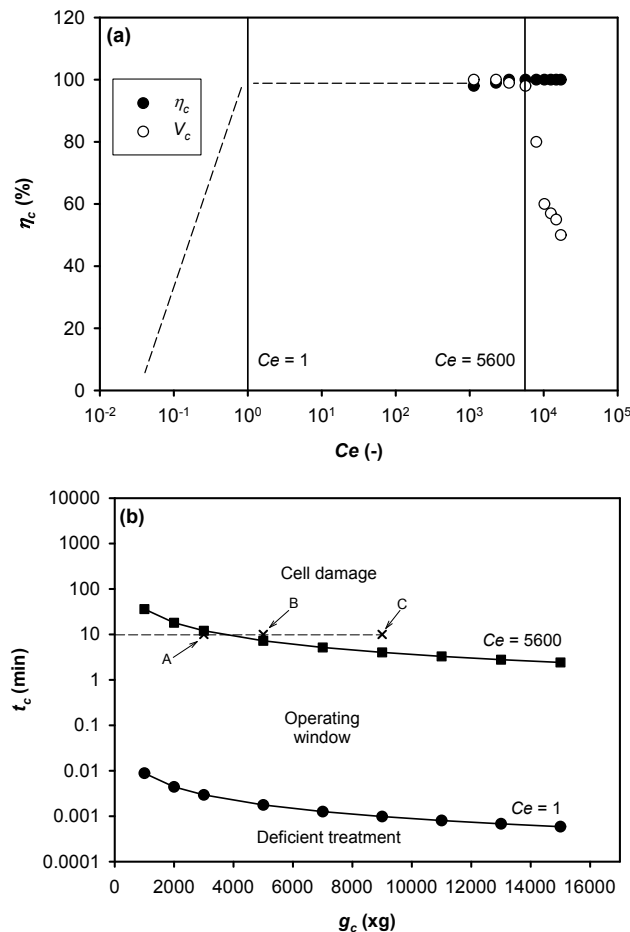
Fig. 5. Separation efficiency (η_c) and cell viability (V_c) for different centrifugation

numbers (*Ce*) (a), and operating window (b), for centrifugation of *D. salina* cells. *Ce* =

21

1 is the *Ce* value for complete cell separation and *Ce* = 5600 is the "critical *Ce*", the *Ce*

value above which cell integrity is compromised. See text for further details.

3.4. Application to Spodoptera exigua cells

In a recent study, Molina-Miras et al. [31] studied the effect of centrifugation on the

Spodoptera exigua Se301 cell line, using the "Excess of Treatment", an intensive

variable, to predict cell damage. Experiments were carried out using 15 mL Falcon

tubes (2.2 cm suspension height) in a benchtop centrifuge (Sigma, model 4-15C) using a

swing-out rotor with a maximum radius of 18.2 cm at g-forces ranging from 20 to

4000×g for different times of up to 45 min. The authors assumed a spherical shape with

a diameter of 18 μm for *S. exigua* and Stokes' law and CFD were used to estimate t_s and

make a comparison with experimental values. The results for *S. exigua* (see Fig. 6) were

similar to those found for *A. carterae* (Fig. 3). Although the deviation from Stokes'

equation is less than with *A. carterae*, this equation underestimated t_s, whereas CFD

provided t_s values similar to the experimental ones. The authors also used CFD to

determine the shear stress magnitude in a conical centrifugation tube, with the highest

shear stress value (7.4×10^{-1} Pa) being obtained at the wall at the bottom of the tube.

This value was well below the breaking shear stress value (233 Pa) previously found for

S. exigua cells in a microfluid flow-concentration device [27]. These results clearly

show that, under the conditions used in that study, *S. exigua* cells were not damaged by

the velocity gradient present in the settling process. These authors concluded that cell

damage correlated with long residence times in the pellet at the bottom of the tube, and

with high centrifugal forces. They were also able to distinguish between mechanical cell

damage at high g-forces and cell damage due to oxygen depletion in the pellet at longer

times [31]. These findings were in accordance with those previously reported by

22

Peterson et al. [29], who observed that compressive forces squeezed the cells against the

tube wall and defined a "Compaction Parameter" to determine the fraction of the pellet

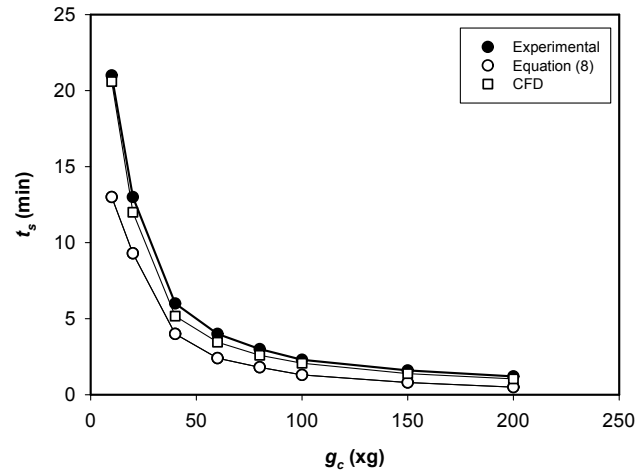that was damaged in a specific centrifugation protocol.

Fig. 6. Influence of g_c on sedimentation time (t_s) for *S. exigua* cells. Experimental times

are taken from reference [31]. Theoretical values of t_s predicted with Eq. (8) and CFD

are also shown.

Application of the *Ce* approach to data for *S. exigua* cells is shown in Fig. 7. Fig. 7a

shows that η_c increases with *Ce* to 100% at a *Ce* value of 1, remaining constant for

higher values of *Ce*. Severe cell damage, with a marked decrease in V_c, was observed

for *Ce* values higher than 3.5. This means that the operating window for this cell type is

very narrow, as can be seen from Fig. 7b and corroborated by the experimental data.

According to the authors, in the experiment carried out at 60×g and t_c = 1 min, the time

that the cells were in the pellet was < 0, with a V_c of 98%. This indicates a deficient

treatment, as can be seen in Fig. 7b (point A). Point B in Fig. 7b represents the

experiment at 400×g and t_c = 1 min. According to the authors, in this experiment all

cells were sedimented and the V_c for the cells in the pellet was 98%. This experiment

23

clearly falls within the operating window. However, when the g-force was increased to

$1000\times g$ with t_c remaining constant (1 min), a decrease in cell viability in the pellet to

90% was observed. This experiment is clearly outside the operating window (point C).

A similar result was observed in the experiment at $400\times g$ and $t_c = 4$ min (point D), with

a decrease in V_c to 91% being observed. However, the most damaging conditions are

represented by point E ($4000\times g$, $t_c = 16$ min), with a decrease in V_c to 60%. Clearly, the

selection of g_c and t_c in this case is highly critical to obtain complete separation and

avoid cell damage.
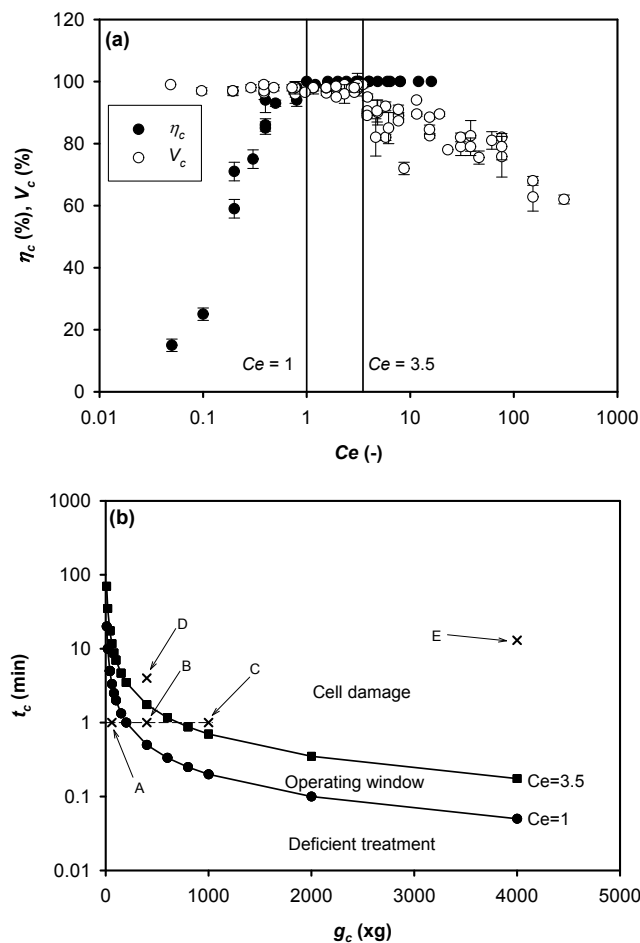
Fig. 7. Separation efficiency (η_c) and cell viability (V_c) for different centrifugation

numbers (Ce) (a), and operating window (b), for centrifugation of *S. exigua* cells. $Ce =$

1 is the Ce value for a complete cell separation and $Ce = 3.5$ is the "critical Ce", the Ce

24

value above which cell integrity is compromised. The separation efficiency and cell

viability data are represented as the average for duplicate experiments ± standard

deviation. See text for further details.

4. Conclusions

In this study, Computer Fluid Dynamics has been successfully used to simulate and

predict the settling time of a single-cell suspension in discontinuous centrifugation. In

addition, the centrifugation number (*Ce*) has been used to obtain an operating window

for *Amphidinium carterae* centrifugation in a discontinuous centrifuge. This approach

has been extrapolated to other cells in benchtop centrifuges and has been shown to

provide an efficient guide for selecting the combination of critical centrifugation

parameters from a cell separation-cell integrity perspective.

Contributions

All authors were involved in the conception and design of the study, acquisition,

analysis, and interpretation of the data, and drafting of the paper. All authors agree to

submission of the final version of the manuscript. A. Contreras-Gómez takes

responsibility for the integrity of the entire work and can be contacted at

acontre@ual.es.

25

References

[1] Coutteau, A., Sorgeloos, P., 1992. The use of algal substitutes and the requirement for live algae in the hatchery and nursery rearing of bivalve molluscs: and international survey. J. Shellfish Res. 11, 467-476.

[2] Razzak, S.A., Hossain, M.M., Lucky, R.A., Bassi, A.S., 2013. Integrated CO_2 capture, wastewater treatment and biofuel production by microalgae culturing-a review. Renew. Sust. Energ. Rev. 27, 622-653.

[3] Christenson, L. and Sims, R., 2011 Production and harvesting of microalgae for wastewater treatment, biofuels, and bioproducts. Biotechnol. Adv. 29, 686-702.

[4] Khan, M. I., Shin, J. H., Kim, J. D., 2018. The promising future of microalgae: current status, challenges, and optimization of a sustainable and renewable industry for biofuels, feed, and other products. Microb. Cell Fact. 17(1), 36.

[5] Assunção, M. F., Amaral, R., Martins, C. B., Ferreira, J. D., Ressurreição, S., Santos, S. D., Varejão, JMTB, Santos, L. M.A., 2017. Screening microalgae as potential sources of antioxidants. J. Appl. Phycol. 29(2), 865-877.

[6] Gallardo-Rodríguez, J., Sánchez-Mirón, A., García-Camacho, F., López-Rosales, L., Chisti, Y., Molina-Grima, E., 2012. Bioactives from microalgal dinoflagellates. Biotechnol. Adv. 30(6), 1673-1684.

[7] Kobayashi, J.i., Kubota, T., 2010. 2.09 - Bioactive Metabolites from Marine Dinoflagellates, in: Liu, H. W., Mander, L. (Eds.), Comprehensive Natural Products II. Elsevier, Oxford, pp. 263-325.

[8] Wang, S., Chen, J., Li, Z., Wang, Y., Fu, B., Han, X., Zheng, L., 2015.
Cultivation of the benthic microalga *Prorocentrum lima* for the production of
diarrhetic shellfish poisoning toxins in a vertical flat photobioreactor.
Bioresour. Technol. 179, 243-248.

[9] López-Rosales, L., García-Camacho, F., Sánchez-Mirón, A., Chisti, Y., 2015.
An optimal culture médium for growing *Karlodinium veneficum*: Progress
towards a microalgal dinoflagellate-based bioprocess. Algal Rech. 10, 177-
182.

[10] Molina-Miras, A., Morales-Amador, A., de Vera, C. R., López-Rosales, L.,
Sánchez-Mirón, A., Souto, M. L., Fernández, J. J., Norte, M., García-
Camacho, F., Molina-Miras, E., 2018. A pilot-scale bioprocess to produce
amphidinols from the marine microalga *Amphidinium carterae*: Isolation of a
novel analogue. Algal Rech. 31, 87-98.

[11] López-Rosales, L., García-Camacho, F., Sánchez-Mirón, A., Beato, E. M.,
Chisti, Y., Grima, E. M., 2016. Pilot-scale bubble column photobioreactor
culture of a marine dinoflagellate microalga illuminated with light emission
diodes. Bioresour. Technol. 216, 845-855.

[12] López-Rosales, L., Sánchez-Mirón, A., García-Camacho, F., Place, A. R.,
Chisti, Y., Molina-Grima, E., 2018. Pilot-scale outdoor photobioreactor
culture of the marine dinoflagellate *Karlodinium veneficum*: Production of a
karlotoxins-rich extract. Bioresour. Technol. 253, 94-104.

[13] Molina-Miras, A., López-Rosales, L., Sánchez-Mirón, A., Cerón-García, M.
C., Seoane-Parra, S., García-Camacho, F., Molina-Grima, E., 2018. Long-
term culture of the marine dinoflagellate microalga *Amphidinium carterae* in

an indoor LED-lighted raceway photobioreactor: Production of carotenoids and fatty acids. Bioresour. Technology. 265, 257-267.

[14] León-Bañares, R., González-Ballester, D., Galván, A., Fernández, E., 2004. Transgenic microalgae as green cell-factories. Trends Biotechnol. 22(1), 45-52.

[15] Badvipour, S., Eustance, E., Sommerfeld, M. R., 2016. Process evaluation of energy requirements for feed production using dairy wastewater for algal cultivation: Theoretical approach. Algal Rech. 19, 207-214.

[16] Chisti, Y., 2007. Biodiesel from microalgae. Biotechnol. Adv. 25(3), 294-306.

[17] Gerardo, M. L. Van Den Hende, S. Vervaeren, H., Coward, T., Skill, S. C., 2015. Harvesting of microalgae within a biorefinery approach: A review of the developments and case studies from pilot-plants. Algal Rech. 11, 248-262.

[18] Molina-Grima E., Belarbi, E. H., Acién-Fernández, F. G., Robles-Medina, A., Chisti, Y., 2003. Recovery of microalgal biomass and metabolites: process options and economics. Biotechnol Adv. 20, 491-515.

[19] Pirwitz, K., Flassig, R. J., Rihko-Struckmann, L. K., Sundmacher, K., 2015. Energy and operating cost assessment of competing harvesting methods for *D. salina* in β-carotene production process. Algal Rech. 2015, 12, 161-169.

[20] Barros, A. I., Gonçalves, A. L., Simões, M., Pires, J. C., 2015. Harvesting techniques applied to microalgae: a review. Renew. Sust. Energ. Rev. 41, 1489-1500.

28

[21] Xu, Y., Milledge, J. J., Abubakar, A., Swamy, R. A. R., Bailey, D., Harvey, P. J., 2015. Effects of centrifugal stress on cell disruption and glycerol leakage from *Dunaliella salina*. Microalgae Biotechnol. 1, 20-27.

[22] Guillard, R.R.L. Ryther, J.H., 1962. Studies of marine planktonic diatoms. I. *Cyclotella nana* Hustedt and *Detonula confervacea* Cleve. Can. J. Microbiol. 8, 229-239.

[23] Guillard, R.R.L., 1975. Culture of phytoplankton for feeding marine invertebrates, in: Smith W. L., Chanley M. H., (Eds.), Culture of Marine Invertebrate Animals. Plenum Press, New York, pp. 26-60.

[24] López-Rosales, L., García-Camacho, F., Sánchez-Mirón, A., Contreras-Gómez, A., Molina Grima, E., 2015. An optimisation approach for culturing shear-sensitive dinoflagellate microalgae in bench-scale bubble column photobioreactors. Bioresour. Technol. 197, 375–382.

[25] Seoane, S., Molina-Miras, A., López-Rosales, L., Sánchez-Mirón, A., Cerón-García, M. C., García-Camacho, F., Madariaga, I., Molina-Grima, E., 2018. Data on the *Amphidinium carterae* Dn241EHU isolation and morphological and molecular characterization. Data Brief. 20, 1-5.

[26] Whitelam, G. C., Lanaras, T., Codd, G. A., 1983. Rapid separation of microalgae by density gradient centrifugation in percoll. Br. Phycol. J. 18(1), 23-28.

[27] Gallardo-Rodríguez, J. J., López-Rosales, L., Sánchez-Mirón, A., García-Camacho, F., Molina-Grima, E., Chalmers, J. J., 2016. New insights into shear-sensitivity in dinoflagellate microalgae. Bioresour. Technol. 200, 699-705.

[28] Fasaei, F., Bitter, J. H., Slegers, P. M., van Boxtel, A. J. B., 2018. Techno-economic evaluation of microalgae harvesting and dewatering systems. Algal Res. 31, 347-362.

[29] Peterson, B. W., Sharma, P. K., van der Mei, H. C., Busscher, H. J., 2012. Bacterial cell surface damage due to centrifugal compaction. Appl. Environ. Microbiol. 78, 120-125.

[30] Maybury, J. P., Hoare, M., Dunnill, P., 2000. The use of laboratory centrifugation studies to predict performance of industrial machines: Studies of shear-insensitive and shear-sensitive materials. Biotechnol. Bioeng. 67(3), 265-273.

[31] Molina-Miras, A., Sánchez-Mirón, A., García-Camacho, F., Molina-Grima, E., 2018. CFD-aided optimization of a laboratory-scale centrifugation for a shear-sensitive insect cell line. Food Bioprod. Process. 107, 113-120.

[32] Häggström, L., 2003. Cell metabolism. Anim. Encycl. Cell Technol. 1, 392-411, http://dx.doi.org/10.1002/0471250570.spi040

[33] Boychyn, M., Yim, S. S. S., Shamlou, P. A., Bulmer, M., More, J., Hoare, M., 2001. Characterization of flow intensity in continuous centrifuges for the development of laboratory mimics. Chem. Eng. Sci. 56(16), 4759-4770.

[34] Geankoplis, C.J., 2003. Transport Processes and Separation Process Principles: (Includes Unit Operations), fourth ed. Prentice Hall, Upper Saddle River, NJ.

[35] Bagheri, G., Bonadonna, C., 2016. On the drag of freely falling non-spherical particles. Powder Technol. 301, 526-544.

[36] Major, J.J., 2003. Hindered settling, in: Middleton, G. W., Church, M. J., Coniglio, M., Hardie, L. A., Longstaffe, F. J. (Eds), Encyclopedia of

Sediments and Sedimentary Rocks. Kluwer Academic Publishers, Dordrecht,

The Netherlands, pp. 358-360.

Conflict of interest

The authors have no conflicts of interest to disclose.